FACTA UNIVERSITATIS
Series: **Automatic Control and Robotics** Vol. 9, N° 1, 2010, pp. 41 - 58

SLIDING MODE CONTROL OF ANTI-LOCK BRAKING SYSTEM: AN OVERVIEW

UDC 681.5.01 62-783.52

Dragan Antić[1], Vlastimir Nikolić[2], Darko Mitić[1], Marko Milojković[1], Staniša Perić[1]

[1]University of Niš, Faculty of Electronic Engineering, Department of Automatic Control, Aleksandra Medvedeva 14, 18000 Niš, Serbia
[2]University of Niš, Faculty of Mechanical Engineering, Aleksandra Medvedeva 14, 18000 Niš, Serbia
E-Mail: dragan.antic@elfak.ni.ac.rs, darko.mitic@elfak.ni.ac.rs, marko.milojkovic@elfak.ni.ac.rs, stanisa.peric@elfak.ni.ac.rs, vnikolic@masfak.ni.ac.rs

Abstract. *An anti-lock braking system control is a rather difficult problem due to its strongly nonlinear and uncertain characteristics. To overcome these difficulties, robust control methods should be employed such as a sliding mode control. The aim of this paper is to give a short overview of sliding mode control techniques implemented in the control of ABS. The most used control algorithms are applied to a quarter vehicle model to demonstrate the advantages of this control approach. Fast convergence and good performances of the designed controllers are verified through digital simulations and validated in real time applications using a laboratory experimental setup.*

Key words: *antilock braking system, wheel slip, sliding mode control*

1. INTRODUCTION

Anti-lock braking system (ABS) is an electronic system helping secure and controlled abrupt stopping of a vehicle. The inventor is Bosch who has been developing this system since the end of the thirties of the last century. The ABS was first used in a series car production in 1978 (S-class Mercedes). Over the next twenty years, it has been significantly improved, and nowadays it represents the standard equipment of the vast majority of modern vehicles. The basic idea of ABS is to prevent the wheels to stop completely during sudden braking. If that happens, the control over vehicle is lost and it can skid in an undesirable direction. ABS does not allow the wheels to be stiffened and thus enables the driver to operate the vehicle normally, although the brake pedal is pressed to the end.

Received November 20, 2010

ABS consists of a hydraulic modulator (control valve), control electronics (central unit) and sensors on the wheels. Sensors constantly acquire information on braking power, although there are no affordable sensors which can accurately identify the road surface, and make this data available to ABS controller. When braking is so intense that it may block the wheel, the controller in the central electronic unit sends the information to the hydraulic system to open the electro-magnetic valves. This reduces the pressure of the oil in the hydraulic system, and consequently the force on the brake disks. As soon as the wheel rotating starts, the sensor sends this information to the controller and it closes the solenoid valves providing the maximum braking force until new wheel relock. The system is designed to repeat this sequence several times during one rotation of the wheel and this is manifested as brake pedal pulsing. As already mentioned, the main objective of the controller is to ensure the best adhesion of the wheel to the surface. This is performed by controlling the road adhesion coefficient.

The road adhesion coefficient is the coefficient of proportion between the friction force, generated during the acceleration and braking phase, and the normal load of the vehicle. It is shown that this coefficient is in nonlinear dependence on the wheel slip, defined as the relative speed difference between the wheel and vehicle. In most papers, ABS controller is designed to regulate the wheel slip so that the road adhesion coefficient has a maximum value. In [1] the desired wheel slip is considered to be constant and the regulator problem is analyzed, while in [2] it is shown that the optimal value of wheel slip should be in the range from 0.08 to 0.3.

ABS mathematical model is not fully developed due to its nonlinear structure, although this system has been used for several decades. System nonlinearities are reflected in unknown parameters of vehicle environment and nonlinear characteristics of braking dynamics. Besides that, the system parameters vary, which is caused by components deterioration, and many external disturbances cannot be predicted in advance. That is why sliding mode control (SMC) methods seem to be the right choice in the control of ABS.

SMC belongs to the well-studied class of discontinuous control systems [3, 4, 5]. Sliding mode is of particular interest in these nonlinear systems and it occurs when the system state is forced to move along a predefined sliding surface, determined by the so-called switching function. If sliding mode exists, a system becomes robust to parameter variations and external disturbances, and its dynamics is known in advance and usually of the low order. The shortcoming of SMC is the existence of the chattering phenomenon. It occurs as the consequence of the high frequency control signal, which can excite the system's unmodelled dynamics.

Traditional SMC enhanced by a grey system theory is proposed in [1], [14]. This theory may deal with uncertain systems which makes it a good candidate for ABS control. In this paper, a grey predictor is used to estimate the angular wheel velocity and linear vehicle velocity. The proposed controller possesses faster convergence and better noise response in comparison to conventional approaches. The wheel slip control through the engine torque control is given in [6]. The moving sliding surface is used to ensure that the system state is always on sliding surface. The chattering problem is discussed in [7], and the integral switching function is introduced to cope with this phenomenon. The integral sliding surface is also used in design of SMC for hybrid electric brake system made from a contact conventional hydraulic brake system and contactless Eddy current brake system [8]. The traditional SMC is implemented in developing of magnetorheological brake

system which is purely an electronically controlled brake system without hydraulics [9]. Digital simulation results of ABS with conventional SMC, where hydraulic brake dynamics is neglected during the design, is shown in [10]. The combination of SMC and the sliding mode observer is elaborated in [11]. First, the SMC is designed to regulate the wheel slip at the desired value, and then, the sliding observer is used to replace the direct state feedback with the estimates of vehicle velocity (wheel velocity). In [12], the SMC, allowing the maximum value of the wheel–road friction force during the braking phase, without *a priori* knowledge of optimal slip, is discussed. This approach treats the ABS SMC design in different manner than the concepts based on separation principle, where the problem is divided into the problem of optimal slip estimation and the problem of tracking the estimated optimal value. The adaptive SMC of vehicle traction is considered in [13]. The proposed control method uses the difference between vehicle and wheel velocities (denoted as slip velocity) as controlled variable instead of the wheel slip representing the relative difference. The adaptive law, estimating the road adhesion coefficient, is combined with the traditional SMC. The overall system stability is proved by using Lyapunov theory. The robust SMC in combination with the neural networks and the moving sliding surface is presented in [15]. The integration of SMC and pulse width modulation (PWM) method, realized by using computer software as opposed to hardware, is given in [16]. This results in quasi continuous control of ABS wheel slip. In [17], the previous approach is analyzed in detail and it is compared with the traditional SMC of wheel slip. The SMC concept is also implemented in hybrid electric vehicle brake system control [18], where a permanent magnet synchronous motor, mounted on wheel shafts through reductors, serves as a generator producing a negative torque to the rear wheels and recovering kinetic energy into electric energy. In [19], the novel nonlinear control with integral feedback is compared with SMC. For overall vehicle stability enhancement, the traditional SMC is also used in wheel slip control [20], while the linear quadratic regulator is exploited for yaw moment controller.

The paper is organized as follows. Section 2 starts with ABS description, then continues with the mathematical model of quarter vehicle describing longitudinal motion of the vehicle and angular motion of the wheel under braking. Section 3 describes the most used SMC approaches in ABS. Digital simulation and experimental results verifying the SMC utilization are presented in section 4. Concluding remarks are given in section 5.

2. ANTI-LOCK BRAKING SYSTEM

A. System description

Consider the system shown in Fig. 1 [22] with two rolling wheels. The lower car-road wheel animates relative road motion while the upper car wheel permanently remains in a rolling contact with the lower wheel. The wheel mounted to the balance lever is equipped in a tire. The car-road wheel has a smooth surface which can be covered by a given material to simulate the road surface.

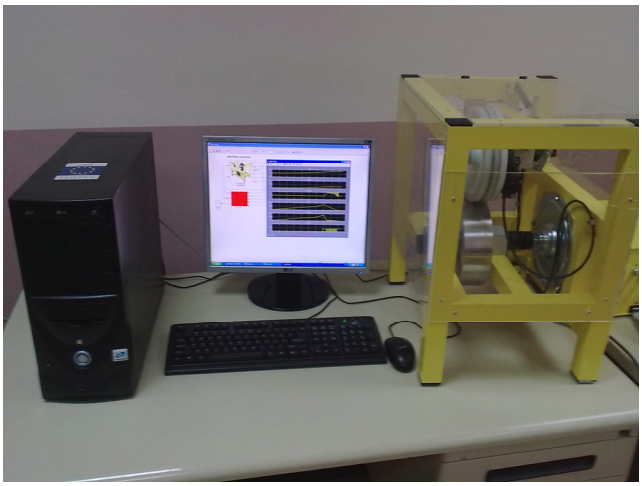

Fig. 1. The ABS system by Inteco

Three angles are measured by encoders with the accuracies of $2\pi/2048 = 0.175°$. While two rotary encoders are installed on both of the wheels to measure the angles, an additional one is used to identify the angular position of the balance lever. The last one might be used in more complex models of ABS. The wheel angular velocities are not measured and they have to be estimated. The simplest Euler formula is used with the sample time period of 0.5 ms.

The upper wheel is equipped in the disk brake system connected via hydraulic coupling to the brake lever which by the tight side and tightening pulley is driven by the small *dc* motor. The lower wheel is coupled to the big flat *dc* motor whose task is to accelerate the wheel. During the braking phase its power supply is switched off. Both *dc* motors are controlled by PWM (pulse-width modulation) signals of the 3.5 kHz frequency.

The power interface amplifies the control signals which are transmitted from the PC to the *dc* motor. It also converts the encoders pulse signals to the digital 16-bit form to be read by the PC. The PC is equipped with the RT-DAC4/USB multipurpose digital I/O board communicates with the power interface. The whole logic necessary to activate and read the encoder signals and to generate the appropriate sequence of PWM pulses to control the *dc* motors is configured in the Xilinx® chip of the RT-DAC4/USB board. All functions of the board are accessed from the ABS Toolbox which operates directly in the MATLAB®/Simulink® and the RTWT toolbox environment.

B. Mathematical model

The diagram of the quarter vehicle model taking into consideration longitudinal motion of the vehicle and angular motion of the wheel is given in Fig. 2. The model is quite simple, since several assumptions are made: only the longitudinal dynamics of the vehicle is considered while the lateral and the vertical motions are neglected, and there is no influence of other vehicle wheels. Despite this model simplification, it preserves the fundamental characteristics of a real system.

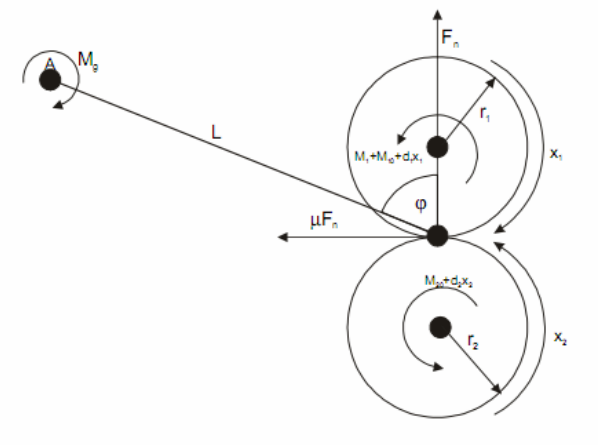

Fig. 2. Free body diagram of ABS

The car velocity is equal to the angular velocity of the lower wheel multiplied by the radius of this wheel, while the angular velocity of the wheel is equal to the upper wheel angular velocity. According to Fig. 2, x_1 represents the angular velocity of the upper wheel, x_2 is the angular velocity of the lower wheel and r_1, r_2 represents the radius of the upper and lower wheel, respectively.

There are three torques acting on the upper wheel: the braking torque M_1, the friction torque in the upper bearing and the friction torque among the wheels and two torques acting on the lower wheel: the friction torque in the lower bearing and the friction torque among the wheels. Besides, we have two more forces acting on the lower wheel: the gravity force of the upper wheel and the pressing force of the shock absorber.

During deceleration, braking torque is applied to the upper wheel, which causes wheel speed to decrease. Introducing the auxiliary variables:

$$s = \mathrm{sgn}(r_2 x_2 - r_1 x_1)\,. \tag{1}$$

$$s_1 = \mathrm{sgn}(x_1)\,. \tag{2}$$

$$s_2 = \mathrm{sgn}(x_2)\,. \tag{3}$$

The motion equation of the upper wheel can be written as:

$$J_1 \dot{x}_1 = F_n r_1 s\mu(\lambda) - d_1 x_1 - s_1 M_{10} - s_1 M_1\,, \tag{4}$$

by using the Newton's second law, where: J_1 is the moment of inertia of the upper wheel, d_1 is the viscous friction coefficient of the upper wheel and M_{10} is the static friction of the upper wheel. As one can see from (4), the friction force is assumed to be proportional to the normal pressing force F_n (the upper wheel acting on the lower wheel). $\mu(\lambda)$ is the coefficient of proportion called the road adhesion coefficient

Similarly, the motion equation for the lower wheel can be defined as:

$$J_2 \dot{x}_2 = -F_n r_2 s\mu(\lambda) - d_2 x_2 - s_2 M_{20}\,, \tag{5}$$

where J_2 is the moment of inertia of the lower wheel, d_2 is the viscous friction coefficient of the lower wheel and M_{20} is the static friction of the lower wheel. In many papers, the normal force F_n is considered to be a constant and its variations are treated as unmodelled dynamics. In that case, (4) and (5) completely determine the dynamics of the quarter vehicle model.

In order to derive the normal force F_n we write the sum of torques corresponding to the point A (Fig. 2) in the following form:

$$F_n L(\sin\varphi - s\mu(\lambda)\cos\varphi) = M_g + s_1 M_1 + s_1 M_{10} + d_1 x_1, \tag{6}$$

yielding:

$$F_n = \frac{M_g + s_1 M_1 + s_1 M_{10} + d_1 x_1}{L(\sin\varphi - s\mu(\lambda)\cos\varphi)}, \tag{7}$$

where M_g represents gravitational and shock absorber torques acting on the balance lever, L is the distance between the contact point of the wheels and the rotational axis of the balance and φ is the angle between the normal in the contact point and the line L.

Substituting (7) in (4) and (5), the model becomes:

$$J_1 \dot{x}_1 = \frac{M_g + s_1 M_1 + s_1 M_{10} + d_1 x_1}{L(\sin\varphi - s\mu(\lambda)\cos\varphi)} \cdot r_1 s\mu(\lambda) - s_1 M_1 - d_1 x_1 - s_1 M_{10}, \tag{8}$$

$$J_2 \dot{x}_2 = -\frac{M_g + s_1 M_1 + s_1 M_{10} + d_1 x_1}{L(\sin\varphi - s\mu(\lambda)\cos\varphi)} \cdot r_2 s\mu(\lambda) - d_2 x_2 - s_2 M_{20}. \tag{9}$$

In the normal operating conditions, the angular velocity of the wheel would match the forward velocity of the car. During the braking and acceleration phases these velocities differs from one another, and their difference is called the wheel slip λ, and it is generally defined as:

$$\lambda = \begin{cases} \dfrac{r_2 x_2 - r_1 x_1}{r_2 x_2}, r_2 x_2 \geq r_1 x_1, x_1 \geq 0, x_2 \geq 0, \\ \dfrac{r_1 x_1 - r_2 x_2}{r_1 x_1}, r_2 x_2 < r_1 x_1, x_1 \geq 0, x_2 \geq 0, \\ \dfrac{r_2 x_2 - r_1 x_1}{r_2 x_2}, r_2 x_2 < r_1 x_1, x_1 < 0, x_2 < 0, \\ \dfrac{r_1 x_1 - r_2 x_2}{r_1 x_1}, r_2 x_2 \geq r_1 x_1, x_1 < 0, x_2 < 0, \\ 1, x_1 < 0, x_2 \geq 0, \\ 1, x_1 \geq 0, x_2 < 0. \end{cases} \tag{10}$$

for all the quarter vehicle model operating conditions. A zero wheel slip means that the wheel velocity and the vehicle velocity are the same, and when the slip is equal to one it tells us that the tire is not rotating and the wheels are skidding on the road surface, i.e., the vehicle is no longer steerable.

The road adhesion coefficient $\mu(\lambda)$ is a nonlinear function of the wheel slip and other physical variables, and one of its models can be determined by the following equation:

$$\mu(\lambda) = \frac{w_4 \lambda^p}{a + \lambda^p} + w_3 \lambda^3 + w_2 \lambda^2 + w_1 \lambda \,. \tag{11}$$

By denoting:

$$S(\lambda) = \frac{s\mu(\lambda)}{L(\sin\varphi - s\mu(\lambda)\cos\varphi)}, \tag{12}$$

and

$$\begin{gathered} c_{11} = \frac{r_1 d_1}{J_1}, c_{12} = \frac{(s_1 M_{10} + M_g) r_1}{J_1}, c_{13} = -\frac{d_1}{J_1}, \\ c_{14} = -\frac{s_1 M_{10}}{J_1}, c_{15} = \frac{r_1}{J_1}, c_{16} = -\frac{1}{J_1}, \\ c_{21} = -\frac{r_2 d_1}{J_2}, c_{22} = -\frac{(s_1 M_{10} + M_g) r_2}{J_2}, \\ c_{23} = -\frac{d_2}{J_2}, c_{24} = -\frac{s_2 M_{20}}{J_2}, c_{25} = -\frac{r_2}{J_2}. \end{gathered} \tag{13}$$

(8) and (9) can be given as:

$$\dot{x}_1 = S(\lambda, x_1, x_2)(c_{11} x_1 + c_{12}) + c_{13} x_1 + c_{14} + (c_{15} S(\lambda, x_1, x_2) + c_{16}) s_1(x_1) M_1 \,, \tag{14}$$

$$\dot{x}_2 = S(\lambda, x_1, x_2)(c_{21} x_1 + c_{22}) + c_{23} x_1 + c_{24} + c_{25} S(\lambda, x_1, x_2) s_1(x_1) M_1 \,. \tag{15}$$

When the brakes are applied, the wheel speed decreases and the force acting on the wheel increases, causing the slippage between the tire and the road surface. The wheel speed will be lower than the vehicle speed, i.e. $r_2 x_2 \geq r_1 x_1$and $x_1 > 0$, $x_2 > 0$, so that the wheel slip is represented by:

$$\lambda = \frac{r_2 x_2 - r_1 x_1}{r_2 x_2}, \tag{16}$$

In that case, since $s = s_1 = s_2 = 1$, $S(\lambda)$ does not depend on x_1 and x_2 anymore, and (14), (15) can be rewritten as:

$$\dot{x}_1 = S(\lambda)(c_{11} x_1 + c_{12}) + c_{13} x_1 + c_{14} + (c_{15} S(\lambda) + c_{16}) M_1 \,, \tag{17}$$

$$\dot{x}_2 = S(\lambda)(c_{21} x_1 + c_{22}) + c_{23} x_1 + c_{24} + c_{25} S(\lambda) M_1 \,. \tag{18}$$

where $S(\lambda)$ is defined in (12).

ABS controller is designed to maintain the vehicle slip at a particular level, where the corresponding friction force (i.e. road adhesion coefficient) reaches its maximum value. That is why we need to determine quarter vehicle model with wheel slip as a controlled variable [21]. Differentiating (16) results in:

$$\dot{\lambda} = -\frac{r_1}{r_2 x_2}\dot{x}_1 + \frac{r_1 x_1}{r_2 x_2^{\,2}}\dot{x}_2 \,. \tag{19}$$

Putting (17) and (18) in (19), finally gives

$$\begin{aligned}\dot{\lambda} = &-\frac{r_1}{r_2 x_2}((S(\lambda)c_{11}+c_{13})x_1 + S(\lambda)c_{12}+c_{14}) + \\ &+\frac{r_1 x_1}{r_2 x_2^{\,2}}(S(\lambda)c_{21}x_1 + c_{23}x_2 + S(\lambda)c_{22}+c_{24}) - \\ &-\frac{r_1}{r_2}\left(\frac{c_{15}S(\lambda)+c_{16}}{x_2} - \frac{c_{25}S(\lambda)x_1}{x_2^{\,2}}\right)M_1\end{aligned} \,. \tag{20}$$

Taking into account that:

$$\lambda = 1 - \frac{r_1 x_1}{r_2 x_2} \Rightarrow x_1 = \frac{r_2}{r_1}(1-\lambda)x_2 \,, \tag{21}$$

(20) can be rewritten in the next form:

$$\dot{\lambda} = f(\lambda, x_2) + g(\lambda, x_2)M_1, \qquad x_2 \neq 0 \,, \tag{22}$$

where

$$\begin{aligned}f(\lambda, x_2) = &-\left(\begin{array}{l}(S(\lambda)c_{11}+c_{13})(1-\lambda) + \\ +\dfrac{r_1}{r_2 x_2}(S(\lambda)c_{12}+c_{14})\end{array}\right) + \\ &+\frac{(1-\lambda)}{x_2}\left(\begin{array}{l}(S(\lambda)c_{21}\dfrac{r_2}{r_1}(1-\lambda)+c_{23})x_2 + \\ +S(\lambda)c_{22}+c_{24}\end{array}\right)\end{aligned} \tag{23}$$

$$g(\lambda, x_2) = -\frac{r_1}{r_2 x_2}(c_{15}S(\lambda) + c_{16} - \frac{r_2}{r_1}c_{25}S(\lambda)(1-\lambda)) \tag{24}$$

3. SLIDING MODE CONTROL

To illustrate the SMC concept in the design of ABS, two algorithms are discussed herein. Both of them are based on the wheel slip dynamics described by (22) and consist of two terms: the relay component ensuring the system state to reach the sliding surface from any initial point and the so-called equivalent control, which keeps the system state on it. The first algorithm is the traditional SMC, representing the simpler form of this robust control [1]. Since the system is of the first order, the switching function is selected as:

$$\sigma = \lambda - \lambda_r \,, \tag{25}$$

where λ_r is the reference wheel slip. The main control design objective is to find control providing $\sigma = 0$ and consequently $\lambda = \lambda_r$. For the system motion in sliding mode $\dot{\sigma} = 0$, the equivalent control is calculated according to:

$$\dot{\sigma} = 0 \Rightarrow \dot{\lambda} = 0 \Leftrightarrow f(\lambda, x_2) + g(\lambda, x_2) M_1^{eq} = 0 , \tag{26}$$

under the assumption that λ_r = const Eq. (26) yields the equivalent control brake torque in the following form:

$$M_1^{eq} = -g(\lambda, x_2)^{-1} f(\lambda, x_2) . \tag{27}$$

The traditional SMC brake torque is then determined as:

$$M_1 = M_1^{eq} - \overline{M}_1 \operatorname{sgn}(\sigma) , \tag{28}$$

where the parameter $\overline{M}_1$ is chosen to satisfy the reaching and existence condition of sliding mode:

$$\sigma\dot{\sigma} < -\eta|\sigma| , \tag{29}$$

providing the final reaching time:

$$t_r < \frac{|\sigma(t=0)|}{\eta} . \tag{30}$$

Eq. (29) can be rewritten as:

$$\sigma\dot{\lambda} < -\eta|\sigma| , \tag{31}$$

and substitution of (22) in (31), taking into account (28) and (27) gives:

$$-g(\lambda, x_2)\overline{M}_1 < -\eta . \tag{32}$$

The sliding motion in system defined by (22) with the control (28) will exist if $\overline{M}_1$ is selected to fulfill the following inequality:

$$\overline{M}_1 > \frac{\eta}{\min(g(\lambda, x_2))} . \tag{33}$$

As we mentioned earlier, the control signal in (28) consists of two terms. The first term, the equivalent control, M_1^{eq} represents the continuous signal based on estimated system parameters. The second term $\overline{M}_1 \operatorname{sgn}(\sigma)$ is the discontinuous control signal with high speed switching in the intersection of state trajectory and sliding surface. In that way, the system trajectory is forced to move always towards the sliding surface and to chatter along it. The chattering is an undesirable phenomenon in the SMC systems, since it may excite unmodelled system dynamics. The simplest way to alleviate the chattering problem, which occurs because of the discontinuous control term, is to replace the signum function with a continuous one:

$$f(\sigma) = \frac{\sigma}{|\sigma| + \delta}, \tag{34}$$

where $\delta \geq 0$, and the control brake torque can be redefined then with:

$$M_1 = M_1^{eq} - \overline{M}_1 f(\sigma). \tag{35}$$

To improve the system accuracy, another algorithm with the integral switching function:

$$\sigma = (\lambda - \lambda_r) + c_1 \int (\lambda - \lambda_r) dt, \tag{36}$$

is suggested. This control algorithm may influence chattering reduction as well [7]. As in the previous case, the equivalent control brake torque is determined from:

$$\dot{\sigma} = 0 \Rightarrow f(\lambda, x_2) + g(\lambda, x_2) M_1^{eq} + c_1(\lambda - \lambda_r) = 0 \tag{37}$$

resulting in:

$$M_1^{eq} = -g(\lambda, x_2)^{-1}(f(\lambda, x_2) + c_1(\lambda - \lambda_r)) \tag{38}$$

The SMC with integral switching function has the same form as (28), and $\overline{M}_1$ is also selected according to (33) in order to establish the sliding motion in the system. When the sliding mode exists in the system, it becomes robust to parameter uncertainty and external disturbances. This robustness is lost when the discontinuous function in control signal (such is a signum function) is replaced by a continuous one (34).

4. DIGITAL SIMULATION AND EXPERIMENTAL RESULTS

For the purposes of the practical verification of the elaborated control methods, the ABS shown in Fig. 1 is considered [22]. The ABS consists of the "Inteco" braking mechanism and open-architecture software environment for real-time control experiments. The ABS supports the real-time design and implementation of advanced control methods using MATLAB and Simulink tools and extends the MATLAB environment in the solution of braking control problems. On the other hand, the integrated software supports: on-line process identification, control system modeling, design and simulation, as well as a real-time implementation of control algorithms. The ABS uses standard PC hardware platforms and MS Windows operating systems. This system has been used in all experiments with four different control methods employed: SMC with or without chattering reduction for traditional and integral switching function. Each figure consists of three subplots representing the responses of wheel and vehicle velocities (speeds), wheel slip and control brake torque, respectively. The reference wheel slip is considered to be constant and $\lambda_r = 0.2$.

Firstly, digital simulations are performed. Figs. 3-6 represent cases where $\overline{M}_1 = 1$. The chattering is not large in Figs. 3 and 4 since the gain is rather small, but the implementation of continuous function (34) gives better results in that sense (Figs. 5 and 6). The integral switching function with $c_1 = 5$ improves the steady-state accuracy, although the transient response is slower as it is expected.

In order to make digital simulation results closer to experimental ones and to show the positive effects of introducing the integral term into the switching function, the digital simulation is executed once more, but with $\bar{M}_1 = 10$. The results are given in Figs. 7-10. It is obvious that the control with (34) alleviates the chattering phenomenon (Figs. 9 and 10).

A series of experiments is done in the previously described real-time framework. $\bar{M}_1$ is chosen to be 10. The results are presented in Figs. 11-14. The unmodelled dynamics is expressed in relation to digital simulation. The chattering reduction by using (34) has no effects any more, since with the continuous function system loses its robust characteristics. The integral switching function slightly improves the system accuracy.

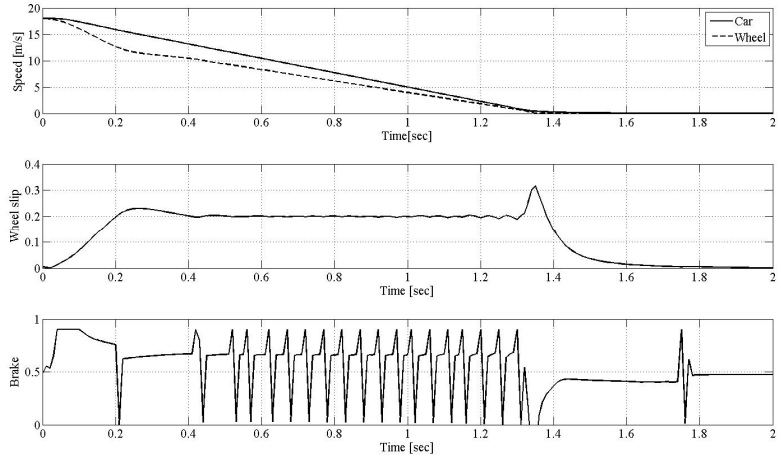

Fig. 3. ABS responses: traditional SMC (simulation results)

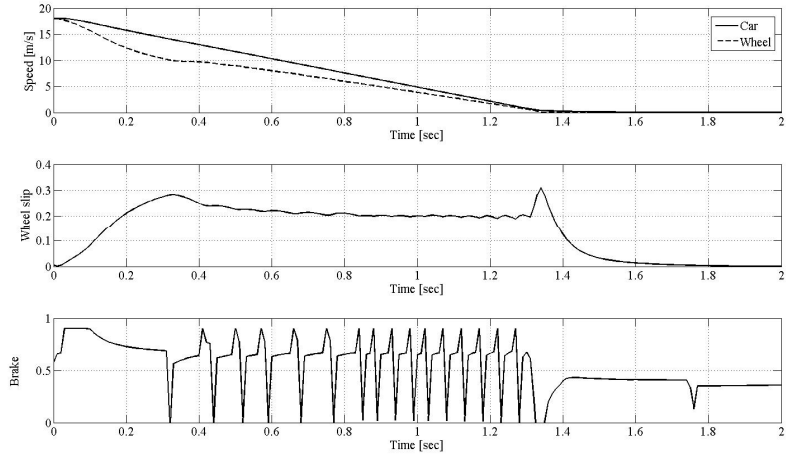

Fig. 4. ABS responses: SMC with integral switching function (simulation results)

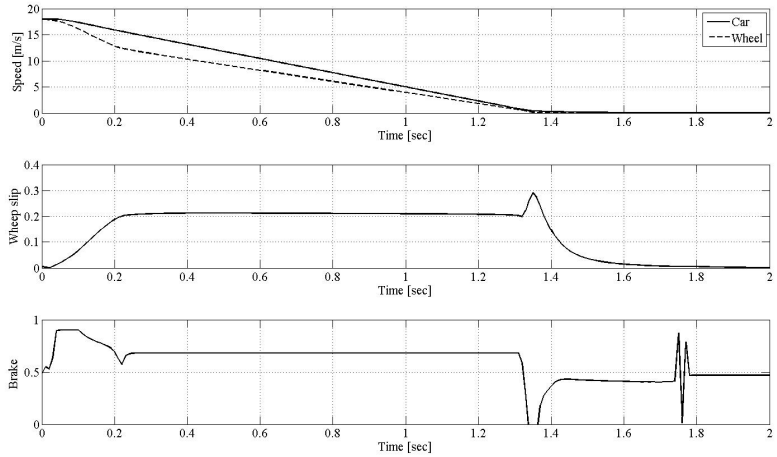

Fig. 5. ABS responses: traditional SMC with chattering reduction (simulation results)

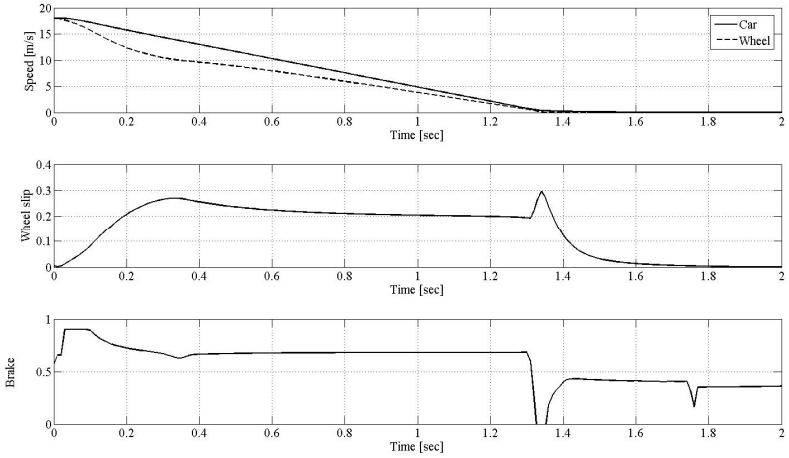

Fig. 6. ABS responses: SMC with integral switching function and chattering reduction (simulation results)

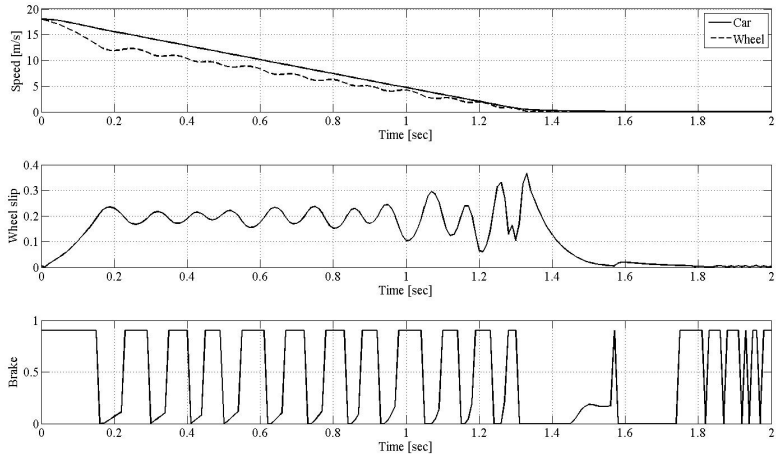

Fig. 7. ABS responses: traditional SMC, $\bar{M}_1 = 10$ (simulation results)

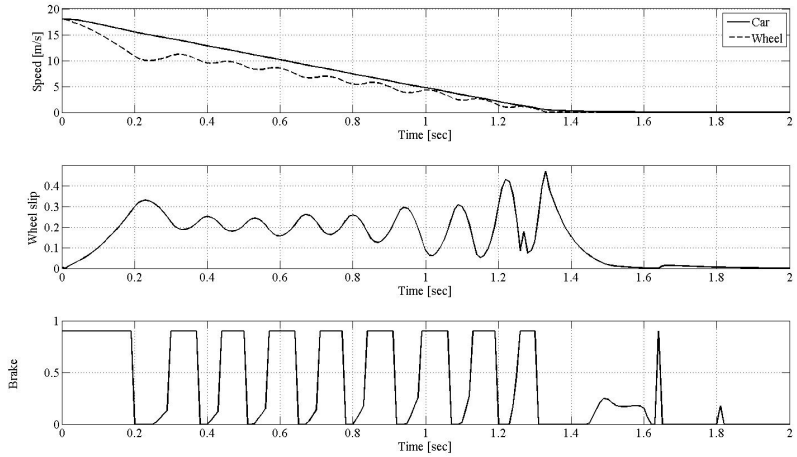

Fig. 8. ABS responses: SMC with integral switching function, $\bar{M}_1 = 10$ (simulation results)

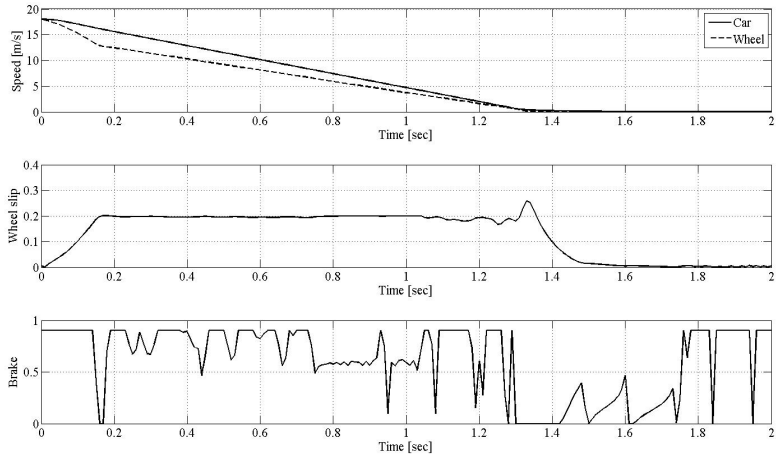

Fig. 9. ABS responses: traditional SMC with chattering reduction, $\bar{M}_1 = 10$ (simulation results)

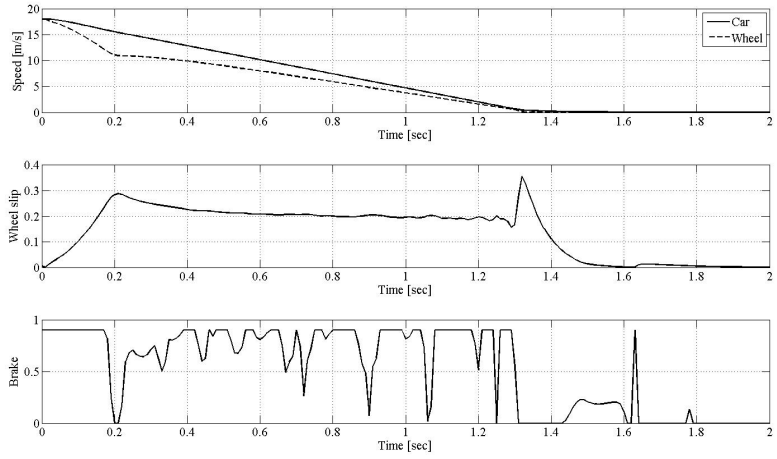

Fig. 10. ABS responses: SMC with integral switching function and chattering reduction, $\bar{M}_1 = 10$ (simulation results)

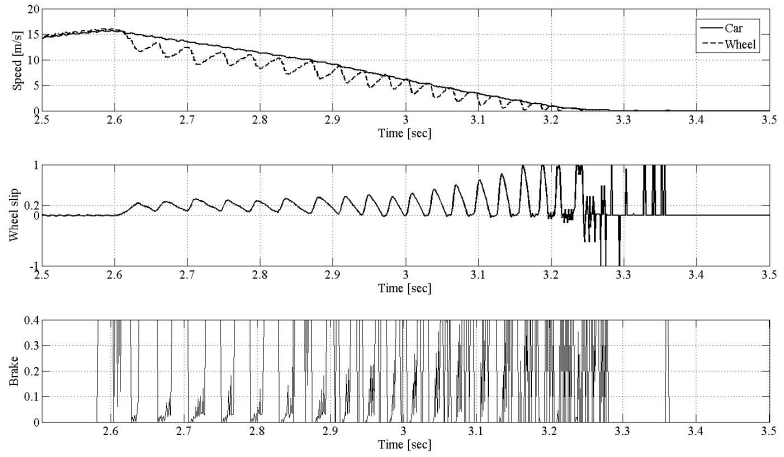

Fig. 11. ABS responses: traditional SMC, $\bar{M}_1 = 10$ (experimental results)

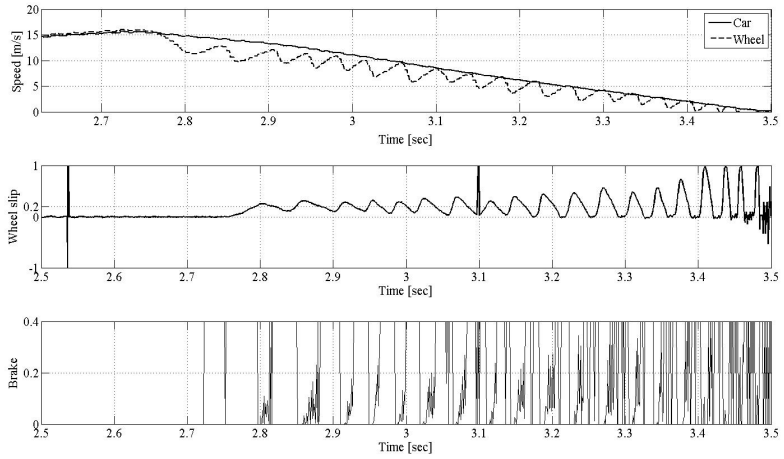

Fig. 12. ABS responses: SMC with integral switching function, $\bar{M}_1 = 10$ (experimental results)

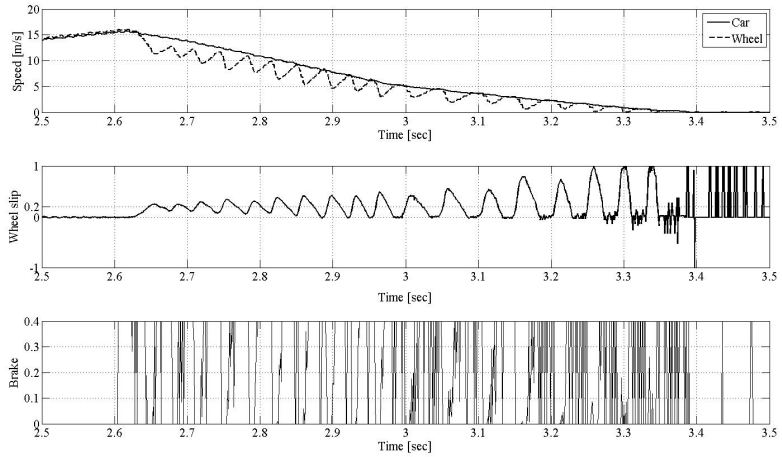

Fig. 13. ABS responses: traditional SMC with chattering reduction, $\bar{M}_1 = 10$ (experimental results)

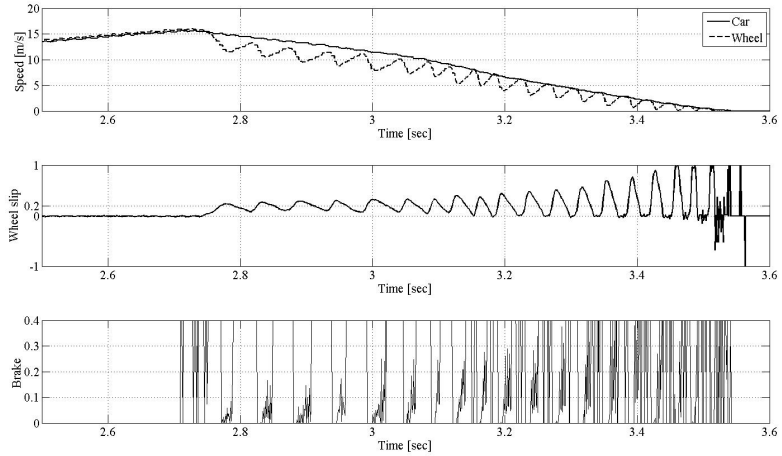

Fig. 14. ABS responses: SMC with integral switching function and chattering reduction, $\bar{M}_1 = 10$ (experimental results)

5. CONCLUSION

In this paper, we give a brief overview of the present solutions in anti-lock braking system control using the sliding mode control techniques. The control algorithms are dominantly designed by using wheel slip model dynamics obtained from the quarter vehicle model. To illustrate the advantages of sliding mode control, a series of digital simulations and real-time experiments are performed for four different control laws, showing that there is great agreement between the obtained theoretical and practical results.

REFERENCES

1. Y. Oniz, E. Kayacan, O. Kaynak, "Simulated and experimental study of antilock braking system using grey sliding mode control", *ISIC. IEEE International Conference on Systems, Man and Cybernetics*, pp. 90-95, 7-10 October 2007.
2. A. Zanten, R. Erhardt, A. Lutz, "Measurement and Simulation of transients in Long-tudinal and Lateral Tire Forces", *SAE Paper*, Vol. 99, No. 6, pp. 300-318, 1990.
3. J. Y. Hung, W. Gao, and J. C. Hung, "Variable Structure Control: A Survey", *IEEE Transactions on Industrial Electronics*, Vol. 40. No. 1, 1993.
4. W. Gao, J. C. Hung., "Variable Structure Control of Nonlinear systems: A New Approach", *IEEE Transactions on Industrial Electronics*, Vol. 40, No. 1, 1993.
5. V. I. Utkin. "Sliding Mode Control Design Principles and Application to Electric Drives", *IEEE Transactions on Industrial Electronics,* Vol. 40, No. 1, 1993.
6. K. Chun, M. Sunwoo, "Wheel slip control with moving sliding surface for traction control system", *International Journal of Automotive Technology*, Vol. 5, No. 2, pp. 123-133, 2004.
7. A. Harifi, A. Aghagolzadeh, G. Alizadeh, M. Sadeghi, "Designing a sliding mode controller for slip control of antilock brake systems", *Transportation Research Part C: Emerging Technologies*, Vol. 16, No. 6, pp. 731-741, December 2008.
8. J. Song, "Performance evaluation of a hybrid electric brake system with a sliding mode controller", *Mechatronics*, Vol. 15, No. 3, pp. 339-358, April 2005.
9. E. J. Park, D.Stoikov, L. Falcao da Luz, A. Suleman, "A performance evaluation of an automotive magnetorheological brake design with a sliding mode controller", *Mechatronics*, Vol. 16, No. 7, pp. 405-416, September. 2006.
10. N. Hamzah, M.Y. Sam, A. A. Basari, "Enhancement of driving safety feature via sliding mode control approach", *Fourth International Conference on Computational Intelligence, Robotics and Autonomous Systems*, pp. 116-120, November 28-30, 2007.
11. C. Unsal, P. Kachroo, "Sliding mode measurement feedback control for antilock braking systems", *IEEE Transactions on Control Systems Technology*, Vol. 7, No. 2, pp. 271-281, March 1999.
12. S. Drakunov, U. Ozguner, P. Dix, B. Ashrafi, "ABS control using optimum search via sliding modes", *IEEE Transactions on Control Systems Technology*, Vol. 3, No. 1, pp. 79-85, March 1995.
13. A. El Hadri, J. C Cadiou, N. K. M'sirdi, "Adaptive sliding mode control of vehicle traction", *15th Triennial World Congress*, July 21-26, 2002.
14. E. Kayacan, Y. Oniz, O. Kaynak, "A grey system modeling approach for sliding-mode control of antilock braking systems", *IEEE Transactions on Industrial Electronics*, Vol. 56, No. 8, pp. 3244-3252, August 2009.
15. Y. Jing, Y. Mao, G. M. Dimirovski, Y. Zheng, S. Zhang, "Adaptive global sliding mode control strategy for the vehicle antilock braking systems", *American Control Conference*, pp. 769-773, June10-12, 2009.
16. M. Wu, M. Shih, "Using the sliding-mode pwm method in an anti-lock braking system", *Asian Journal of Control*, Vol. 3, No. 3, pp. 255-261, September 2001.
17. M. Wu, M. Shih, "Simulated and experimental study of hydraulic anti-lock braking system using sliding-mode PWM control", *Mechatronics*, Vol. 13, No. 4, pp. 331-351, May 2003.
18. X. Yu, G. Li, "Hybrid electric vehicle brake system control metrics design and application", *Proceedings of the International Symposium on Intelligent Information Systems and Applications (IISA'09)*, pp. 174-178, October 28-30, 2009.
19. H. Mirzaeinejad, M. Mirzaei, "A novel method for non-linear control of wheel slip in anti-lock braking systems", *Control Engineering Practice*, Vol. 18, No. 8, pp. 918-926, August 2010.
20. S. Zheng, H. Tang, Z. Han, Y. Zhang, "Controller design for vehicle stability enhancement", *Control Engineering Practice*, Vol. 14, No. 12, pp. 1413-1421, December 2006.
21. D. Antić, V. Nikolić, D. Mitić, M. Milojković, S. Perić, "Sliding mode control of anti-lock braking system: An overview", *X Trienal International SAUM Conference on Systems, Automatic Control and Measurements, SAUM 2010*, *Niš*, *Serbia*, pp. 41-48, November 10-12, 2010.
22. Inteco, "The laboratory Anti-lock Braking System controlled from PC"-*User's Manual*, (2008) available at www.inteco.com.pl.

UPRAVLJANJE ABS SISTEMOM POMOĆU KLIZNOG REŽIMA: PREGLED

Dragan Antić, Vlastimir Nikolić, Darko Mitić, Marko Milojković, Staniša Perić

Upravljanje ABS sistemom je veoma težak problem zbog njegovih izrazito nelinearnih i neizvesnih karakteristika. Da bi se prevazišli ovi problemi, treba da se upotrebe robusne metode upravljanja kao što su upravljanja uz pomoć kliznih režima. Cilj ovog rada je da pruži kratak pregled tehnika upravljanja uz pomoć kliznih režima koje se primenjuju u kontroli ABS sistema. Najčešće upotrebljavani upravljački algoritmi primenjuju se na model četvrtine vozila kako bi se pokazale prednosti ovog pristupa upravljanja. Brza konvergencija i dobre performanse dizajniranih kontrolera su verifikovani kroz digitalne simulacije i provereni su na aplikacijama u realnom vremenu koristeći laboratorijsku eksperimentalnu opremu.

Ključne reči: *ABS sistem, proklizavanje točka, klizni režim*